Suspended Particulate Matter (SPM) mapping from MERIS imagery.
Calibration of a regional algorithm for the Belgian coastal waters

B. Nechad, V. De Cauwer , Y. Park and K. G. Ruddick

Management Unit of North Sea Mathematical Model (MUMM)
100, Gulledelle 1200 Brussels, Belgium
b.nechad@mumm.ac.be, y.park@mumm.ac.be, k.ruddick@mumm.ac.be

ABSTRACT

A hydro-optical algorithm based on reflectance at 555nm has been used in the past for suspended particulate matter concentrations (SPM) retrieval from SeaWiFS over the Belgian coastal (case II) waters in Southern North Sea. The extra spectral resolution of MERIS offers the possibility of improvements, though necessitates algorithm recalibration. This study presents the calibration of the hydro-optical model used to derive SPM from MERIS reflectance for Belgian coastal waters. The model is based simply on reflectance at one suitably-chosen band. Regression analysis is carried out for seaborne measurements of reflectance and SPM taken over our region of interest, to determine and calibrate the bands best suited for SPM detection. Sensitivity of the method to errors is studied.

1   INTRODUCTION

Suspended particulate matter concentration (SPM) mapping using satellite imagery is necessary to provide initial boundary conditions and validation data to sediment transport models [1]. The high spectral resolution of MERIS will enable SPM mapping with more accuracy since the use of red and near infrared bands reduces errors in SPM retrieval which may arise from variations in absorption of phytoplankton, Coloured Dissolved Organic Matter (CDOM) and non algal particles. The objective of this study is to design a regional algorithm for mapping SPM over the Belgian coastal waters from the high spectral resolution MERIS imagery.

The relationship between inherent optical properties (IOPs) and the water surface reflectance was investigated by [2] and is expressed by:

$$R_- = Q\left[l_1 \frac{b_b}{a+b_b} + l_2\left(\frac{b_b}{a+b_b}\right)^2 \right] \qquad (1)$$

where R_- is the subsurface irradiance reflectance defined by $R_- \equiv E_u(0^-)/E_d(0^-)$ where $E_u(0^-)$ and $E_d(0^-)$ are respectively the upward and the downward irradiance just beneath the sea surface; a is the total absorption coefficient and b_b the total backscatter coefficient. The coefficients $l_1=0.095$, $l_2=0.079$ are derived from radiative transfer simulations [2] to relate R_-/Q to a and b_b . Q is the ratio of the upwelling radiance to the zenith-upwelling irradiance.

The coefficients a and b_b may be expressed as the sum of M water constituent inherent optical properties (IOP), where each is linearly related to its concentration by its specific IOP. Equation (1) can be written for each sensor spectral band, in terms of M unknown concentrations. Analytical or semi-analytical methods can be employed to resolve these equations for the desired water quality parameters: SPM, chlorophyll and CDOM. Analytical methods are based on the inversion of the physical model, for example by minimising the χ^2 error, between the measured and the modelled reflectance (e.g. the MERIS standard product [3]).

In this study, a semi-analytical method is used to calibrate a regional algorithm estimating SPM from MERIS reflectance over the Belgian coastal waters. For that a use non-linear regression analysis is made of SPM and ρ_w measurements, sampled during BELGICA and Zeeleeuw campaigns from 2001 to 2003.

The MERIS reflectance is defined by:

$$\rho_w \equiv \pi \frac{L_w(0^+)}{E_d(0^+)} \qquad (2)$$

where $L_w(0^+)$ is the upwelling radiance, and $E_d(0^+)$ is the downwelling irradiance just above the water surface. It can be expressed in terms of the subsurface irradiance reflectance as follows (from [4]):

$$\rho_w = \pi \frac{R_-}{1 - r R_-} \frac{t_{w \to a} t_{a \to w}}{Q n_w^2} \qquad (3)$$

where:

● $t_{w \to a}$ is the bidirectional radiance transmittance from the water to the air, for a sun at zenith $t_{w \to a} \approx 0.98$;

● $t_{a \to w}$ is the irradiance transmittance from the air to the sea, a typical value is $t_{a \to w} \approx 0.96$, for the sun zenith angle <60° in clear or overcast skies;

● $n_w \approx 1.34$ is the real part of the refractive index of water;

● $r R_-$ represents the internal reflectance of the upwelling irradiance, r being the water-air reflectance for totally diffuse irradiance. This should not be neglected for high reflectance occurring in case II waters. Here we use $r=0.48$ from [2].

● For case 2 waters the Q-factor varies with the sun zenith angle and the volume scattering function and with wavelength. It was considered to range from 2.7 to 4.6 sr for high vs low sun [5]. Here we will use an average value $Q=3.7$ sr though we note that the model used has very little sensitivity to this input.

Setting $\alpha \equiv \dfrac{\pi t_{w \to a} t_{a \to w}}{Q n_w^2}$, from above $\alpha \approx 0.52 \dfrac{\pi}{Q}$. The inversion of (3) will be written as:

$$R_- = \frac{\rho_w}{\alpha + r \rho_w} \qquad (4)$$

The hydro-optical model of [2] links the subsurface irradiance reflectance to the inherent water optical properties a and b_b. For 89% of our $\rho_{w=}$ dataset, where ρ_w does not exceed 0.09 for any band, the error associated with the second order term of (1) does not exceed 16%, 24% and 10% respectively in the blue-green, red and near infrared bands. This term is therefore neglected here and (1) becomes:

$$R_- = Q l_1 \frac{b_b}{a + b_b} \qquad (5)$$

b_b is related to SPM concentration (denoted by S) via $b_b = S b_{bs}^*$ (6)

where b_{bs}^* is the specific backscatter coefficient. Substituting this for b_b in (5) and inverting this equation gives:

$$S = \frac{a}{b_{bs}^*} \frac{R_-}{Q l_1 - R_-} \qquad (7)$$

We define the factors A_Q and C_Q as:

$$A_Q \equiv \frac{a}{b_{bs}^* (1 - r Q l_1)} \ , \ C_Q \equiv \frac{0.52 \, \pi l_1}{1 - r Q l_1} \qquad (8)$$

and substitute (4) in (7), leading to:

$$S = A_Q \frac{\rho_w}{C_Q - \rho_w} \qquad (9)$$

2   Data sets

68 ρ_w reflectance spectra were acquired during *Belgica* and Zeeleeuw cruises during 2001-2003 [6], using a system of three Trios spectroradiometers with 2.5nm resolution covering the spectral bandwidth [350nm-950nm]. Since MERIS bands are narrow we interpolate ρ_w for the 15 MERIS band central wavelengths ranging from 412nm to 900nm. For SeaWiFS the reflectance ρ_w^K is computed for each band K with a band width ΔK using the spectral response $\sigma(\lambda)$ of SeaWiFS as follows:

$$\rho_w^K = \frac{\int\limits_{\Delta K} \rho_w(\lambda)\sigma(\lambda)d\lambda}{\int\limits_{\Delta K} \sigma(\lambda)d\lambda} \qquad (10)$$
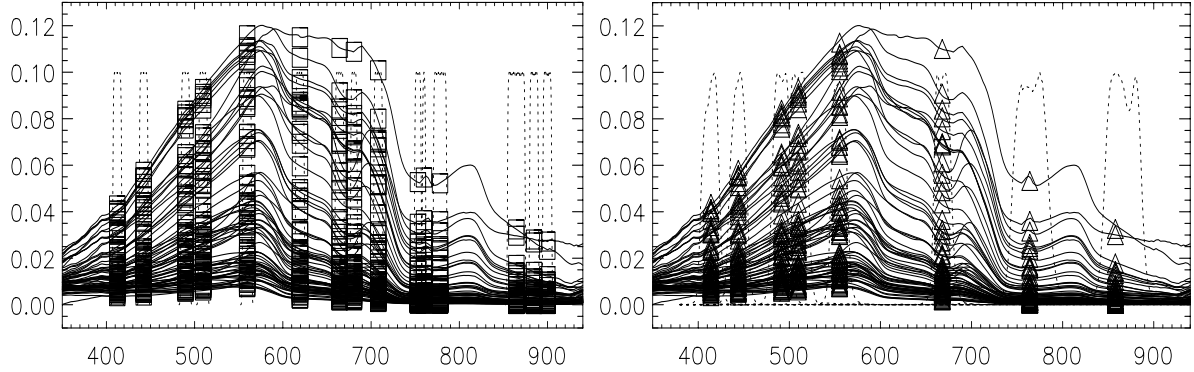
Fig. 1. Reflectance spectra recorded by the Trios system and the derived MERIS (resp. SeaWiFS) spectra plotted by squares in the left (resp. triangles in the right) figure. The sensor response functions are given as dashed lines.

SPM measurements were made at 3m depth, and using a GF/C filter. Fig (2) shows their frequency distribution. Note the isolated observation of 178.4mg/l recorded at station MH6 (51°52.278',1°27.405') during the Belgica campaign of 16.04.2002. At this location the highest reflectance spectrum, reaching 0.12 around 570nm, was recorded.
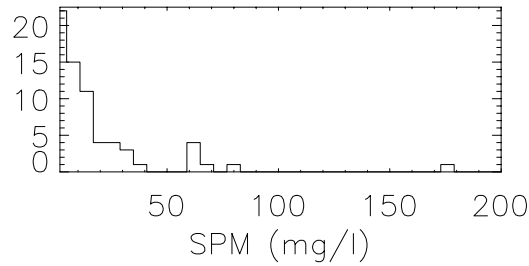
Fig. 2. The distribution of SPM measurements used in this study.

3 NON LINEAR REGRESSION ANALYSIS

Regression analysis will determine the optimal parameter A_Q in the non linear equation (9) for which the curve plot fits best the observations. We modify this equation to allow for measurement and model errors, by adding a second coefficient B:

$$\widehat{S} = A_Q \frac{\rho_w}{C_Q - \rho_w} + B \qquad (11)$$

For the N seaborne measurements of S_i and ρ_w^i, $i=1...N$, where N is the number of observations, model estimates are denoted by $\widehat{S}_i$ and the mean value of S_i by $\overline{S}$. We define the residual or error sum of squares, *SSE,* and the coefficient of multiple determination, R^2, respectively by:

$$SSE \equiv \sum_{i=1}^{N} \left(S_i - \widehat{S}_i\right)^2 \qquad (12)$$

$$R^2 \equiv 1 - \frac{SSE}{\sum\limits_{i=1}^{N}\left(S_i - \overline{S}\right)^2} \qquad (13)$$

R^2 indicates the fraction of variance in the observations set (S_i) that is explained by the regression model and may vary from 0 to 1. $R^2=1$ means the curve fits all data points. The coefficient A that minimizes SSE, corresponding to the highest R^2, is selected for our algorithm calibration. Nevertheless, such a regression analysis is appropriate only when sample variance does not depend on data value and remains constant over the data ranges. However, here S_i is *homoscadastic* i.e. variance increases with increasing ρ_w^i. [7] reported that SPM are log-normally distributed for the Southern North Sea. Hence, log(SPM) are more likely to stabilize the dependent variable S_i variance [8]. We re-formulate the multiple determination coefficient of the regression defined in (13) using the log-transformation:

$$SSE_{log} = \sum\limits_{i=1}^{N}\left(\log(S_i) - \log(\widehat{S}_i)\right)^2 \text{ and } R^2 = 1 - \frac{SSE_{log}}{\sum\limits_{i=1}^{N}\left(\log(S_i) - \sum\limits_{j=1}^{N}\frac{\log(S_j)}{N}\right)^2} \qquad (14)$$

Since the contribution of certain bad points hugely increases the SSE_{log} value, it is necessary to study the distribution of residuals to determine which observations are to be considered as "outliers" to be removed. To objectively identify outliers we examine the statistical parameter: *jackknife residual* [8] for each observation. The Schematic plot of jackknife residuals pointed out 8 (respectively 6) outliers for the models adapted to MERIS bands (respectively to SeaWiFS bands). The highest reflectance value recorded at station MH6 was considered as an outlier by the jackknife algorithm because it is an extreme observation. However, this measurement seams to be coherent with the highest SPM value recorded here (see section 2), so it will not be removed from the regression analysis. Except for this observation all the 7 outliers (resp. 5) were removed.

4   RESULTS

For this MERIS (respectively SeaWiFS) SPM-algorithm, the regression analysis coefficients for the best fitting curves are given in table 1 (respectively table 2) plus the *Bias* and the mean relative error ε_r defined by:

$$Bias = \frac{\sum\limits_{i}^{N}(S_i - \widehat{S}_i)/S_i}{N}, \ \varepsilon_r = \frac{\sum\limits_{i}^{N}\left| S_i - \widehat{S}_i \right|/S_i}{N}$$

Fig. 3 and 4 show the model curves. We note that for higher wavelength bands (> 750nm) no ρ_w measurements exceed the value $\rho_w^i = 0.09$ and the approximation (5) applies better. However, the signal to noise ratio may be less favorable in these bands than in lower wavelengths such as the MERIS band 708nm. For our data sets the mean value of the ratio $\rho_w^{753}/\rho_w^{708}$ is about 0.34.
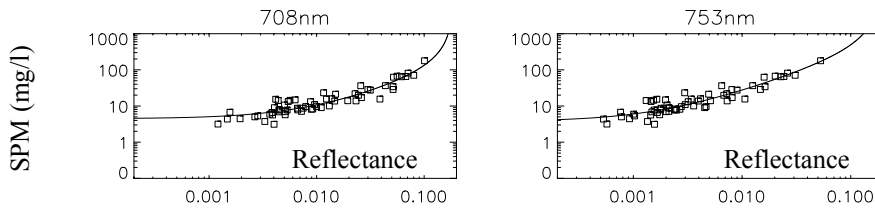
Fig. 3. The SPM measurements *vs* reflectance data scatterplot with the model curves for the 9th and the 10th MERIS bands.
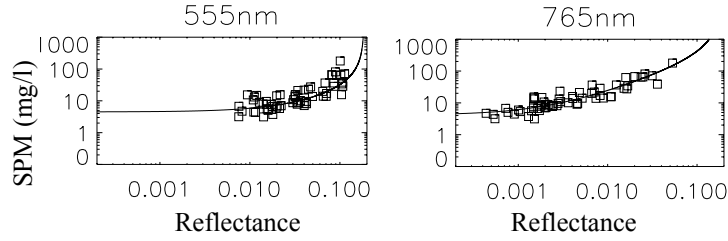
Fig. 4. The SPM measurements *vs* reflectance data scatter plot with the model curves for the 5th and the 7th SeaWiFS bands.

Table 1: MERIS-SPM retrieval models for band 708nm and 753nm.

Wavelengths (nm)	A_Q(mg/l)	B_Q(mg/l)	R^2 (%)	Bias (%)	ε_r (%)
708	111.21	4.46	85.49	5.54	26.13
753	421.87	3.74	84.55	5.80	26.04

Table 2: SeaWiFS-SPM retrieval models for the 5th and the 7th bands.

Wavelengths (nm)	A_Q(mg/l)	B_Q(mg/l)	R^2 (%)	Bias (%)	ε_r (%)
765	360.26	4.16	82.96	6.64	28.89
555	25.55	4.50	67.37	12.64	43.99

5   PRELIMINARY VALIDATION FOR MERIS

At the moment of this study we have only 3 good match-up MERIS images from which 5 good quality reflectance spectra were extracted. Comparison with seaborne SPM measurements yields an average relative error of estimation of about 35% for the MUMM 708nm regional algorithm (resp. 41% for the 753nm model), while the SPM MERIS product gives 63% relative error. However, more data are required for a valid comparison of these two products.

6   SEAWIFS ALGORITHM VALIDATION

9 SeaWiFS images have been analysed with match-up seaborne data at 23 locations. The validation of the algorithm gives a mean relative error of estimates of 36.4% with 78% correlation. This model is better than a previous model (unpublished) used to estimate SPM from SeaWiFS band 5 over the Belgian waters via:

$$\widehat{S} = 41.22 \frac{R^{555nm}_-}{0.33 - R^{555nm}_-}$$

The relative error of estimation was 45.49% and the correlation about 60%. Both models are plotted in Fig.5 and superimposed with SPM *vs* reflectance measurements.

7   DISCUSSION

The impact of ρ_w errors is examined through the following relationship derived from Eq. 9: $\dfrac{\partial S}{S} = \dfrac{\partial \rho_w}{\rho_w} \dfrac{C_Q}{(C_Q - \rho_w)}$

Except for very high reflectance $\rho_w << C_Q \approx 0.187$ and for $S > B$ (4.5mg/l) relative errors in reflectance generate relative errors in SPM with the same magnitude because of linearity of Eq.(11). For very turbid waters as for our dataset, the reflectance reaches 0.1 in band 708nm, yielding a relative error in SPM about 2.25 times the relative error in the reflectance, whereas in band 753nm the lower reflectance ($\rho_w < 0.06$) enables the model to yield lower relative errors for SPM estimates. On the other hand, the model sensitivity to errors in band 708nm is 3 times lower than its sensitivity to errors in band 753nm reflectance (see section 4). As a balance, we may use the band 708nm model to

estimate SPM in *clear to turbid waters* and apply the 753nm model for very turbid waters to avoid errors in the non-linear part of the 708nm model (high reflectance range) and the errors due to the water vapour correction.

In conclusion, the 753nm MERIS band model is well adapted for the turbid Belgian coastal waters, but for clearer waters ($S<4.5$mg/l) this model should be extended.
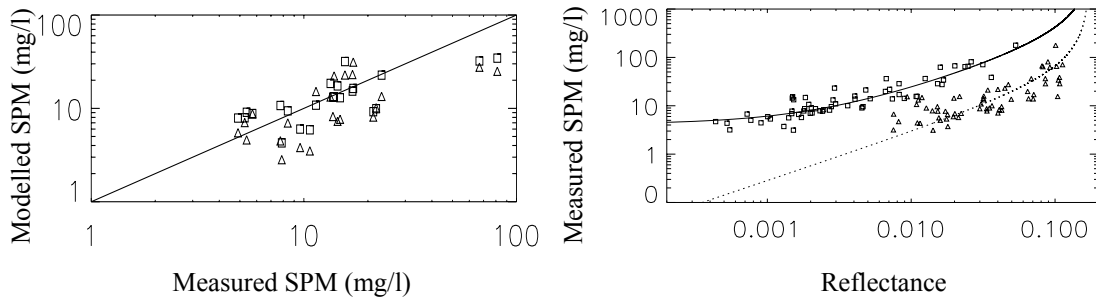
Fig. 5. On the Left: the squares show SPM retrieved from ρ_w data at 765nm and the triangles mark SPM estimated from a previous model using R^{0-} at 555nm. On the right: The scatter plot of measured SPM vs reflectance data at band 765nm (squares) and band 555nm (triangles). The solid line shows the $\rho_w^{(765nm)}$ model and the dotted line the $R^{0-(555nm)}$ model.

9 REFERENCES

1. Fettweis, M. and Van den Eynde, D. The mud deposits and the high turbidity in the Belgian-Dutch coastal zone, Southern bight of the North Sea. *Continental Shelf Research*, 23, 669-691, 2003.

2. Gordon, H.R., O.B. Brown, R.H. Evans, J.W. Brown, R.C. Smith, K.S. Baker, D.K. Clark. A semianalytical radiance model of ocean color. J. G.R.Vol. 93, No. D9, pp. 10 909-10 924,1998.

3. Doerffer,R., H. Schiller. Pigment index, sediment and gelbstoff retrieval from directional water leaving reflectances using inverse modelling technique. (ATBD) 2.12, 1997.

4. Mobley, C.D., Applied Electromagnetics and Optics Laboratory- SRI Int. Light and Water-Radiative transfer in natural waters. Academic press, Inc, 1994.

5. Gons, H.J. Optical teledetection of chlorophyll a in turbid inland waters. Environ. Sci. & Tehcnol, Vol 33. p. 1127-1132, 1999.

6. Ruddick, K.G., V. De Cauwer, Y. Park, G.Becu, J-P. De Blauwe, E. De Vreker, P-Y. Deschamps, M. Knockaert, B. Nechad, A. Pollentier, P. Roose, D. Saudemont, D. Van Tuyckom, Preliminary validation of MERIS water products for Belgian coastal waters in Proceedings of Envisat Validation Workshop 2002, ESA SP-531 (CDROM), 2003

7. Ruddick, . F. Ovidio, D. Van den Eynde and A. Vasilkov. The distribution and dynamics of suspended particulate matter in Belgian coastal waters derived from AVHRR imagery. The 9th Conference on Satellite Meteorology & Oceanography, Paris, France, 25-29 May 1998.

8. Kleinbaum, D.G, L.L. Kupper, K.E. Muller. Applied regression analysis and other multivariable methods. 2nd Edition - PWS-KENT Publishing Compagny, 1998.

8 ACKNOWLEDGEMENT